ANALYTICAL MODELING AND EXPERIMENTAL VALIDATION OF LOW-VELOCITY IMPACT RESPONSES IN UNIDIRECTIONAL CFRP COMPOSITE USING FSDT AND TDOF APPROACHES.

Abdelmunem Bushra Abdalla[1,2], Haris Ahmad Israr[1*], Muhammad Irfan Naufal[1], Mohd Nasir Tamin[1] and Zaini Ahmad[1]

[1]Faculty of Mechanical Engineering, Universiti Teknologi Malaysia, 81310 UTM Johor Bahru, Johor, Malaysia
[2]Aeronautical Research & Development Center, Alsafya Ingaz St, Khartoum, Sudan

[*]Corresponding email: harisahmad@utm.my

Article history
Received
9th March 2025
Revised
21st August 2025
Accepted
23rd August 2025
Published
1st December 2025

ABSTRACT

Metallic structures have been extensively replaced with carbon fiber-reinforced polymer (CFRP) composites in many industries due to their technical advantages and design versatility. Despite these advantages, CFRP composites are sensitive to dynamic loads such as low velocity impact, which can compromise structural integrity with internal damage. This study introduces a computationally efficient analytical model developed in MATLAB to predict impact damage in unidirectional (UD) CFRP composites, providing a faster and more cost-effective alternative to finite element simulations. The model used First Order Shear Deformation Theory (FSDT) and a Two Degrees of Freedom (TDOF) approach, incorporating a nonlinear contact force model to calculate displacements, absorbed energy and impact forces. A key novelty of this research lies in the multi-level experimental validation conducted with an Instron CEAST 9350 impact testing machine with hemispherical impactor tips at energy levels of 5.6 J, 10.3 J and 16.14 J. Results reveal that the model achieves good agreement with experimental data at lower energy levels, accurately captures the elastic behavior with a minimum error of 1%. However, the model's limitations in simulating nonlinear responses and material damage become more evident at higher energy levels, where the extent of damage has a pronounced effect on energy absorption and dissipation. This underscores the need for incorporating advanced material models that account for damage progression and strain-rate effects to enhance accuracy and reliability. Ultimately, this work supports the development of innovative composite solutions, contributing to more efficient and cost-effective engineering practices.

Keywords: *CFRP, low velocity impact, energy absorption, analytical model, structural integrity*

1.0 INTRODUCTION

Carbon fiber-reinforced polymer (CFRP) composites have become indispensable in modern industrial engineering due to their exceptional strength-to-weight ratios, high stiffness, and versatility in design [1-4]. These materials are extensively used in primary and secondary structures across aerospace and automotive sectors, where weight savings are critical without compromising structural integrity [5-6]. The use of CFRP composites

in aerospace applications significantly enhances performance and fuel efficiency, contributing to reduced emissions and operational costs [7], while in the automotive industry, CFRP composites are pivotal for achieving lightweight designs without compromising safety and durability [8]. The anisotropic nature of CFRP composites allows for the customization of mechanical properties to meet specific design requirements, offering flexibility not achievable with traditional materials [9-10].

Despite these advantages, CFRP composites are highly sensitive to dynamic loads, particularly low-velocity impacts (LVI), which can cause significant internal damage that is often not visible on the surface [11]. Such hidden damage can severely compromise the structural integrity and safety of composite structures. Thus, making it crucial to understand and predict the impact behavior of these materials for reliable application in safety-critical environments [12-13]. For that reason, numerous studies on the impact damage of CFRP composites have been reported in the open literature. These investigations encompass a wide range of investigations such as the effects of hybridization [14-15], impactor diameter [16], damage assessment methods [17], laminate design configurations [18], etc. Moreover, current studies are focusing more on the development of finite element modelling [19-21] to accurately predict the low velocity impact problems. Nevertheless, many of these existing finite element models fail to account for damage progression and often require extensive computational resources and calculation time. Analytical models on the other hand could offer a computationally efficient alternative to finite element simulations. This approach enables faster predictions, making it a viable alternative for early-stage design assessments and preliminary structural evaluations. Literary wise, there are limited studies that have been reported related to the development of analytical model to predict impact behavior of CFRP composites.

Analytical models play a vital role in predicting the impact behavior of composite materials, offering a cost-effective and time-efficient alternative to extensive experimental testing. These models could be used by the engineers and designers in assessing the performance of composite structures under various loading conditions, optimizing material selection, and improving design methodologies. However, accurately predicting complex failure mechanisms and energy absorption characteristics under impact remains challenging [22-23]. Li et al developed an analytical model to predict the penetration and non-penetration behaviors cylindrical shells made of fiber-reinforced composite using the critical impact velocity criterion [22]. On the other hand, Singh et al established an analytical model to predict the behavior of carbon/epoxy-aluminum honeycomb core sandwich structures when subjected to quasi-static indentation loading [23]. Both analytical models developed in [22-23] demonstrated good agreements with experimental results despite dealing with complex failure mechanisms and responses. However, the applicability of both models is limited to a specific domain of validity.

This study aims to validate an analytical model developed in MATLAB for predicting impact damage in CFRP composites. The model utilizes First Order Shear Deformation Theory (FSDT) and a Two Degrees of Freedom (TDOF) approach to calculate displacements, energy, and impact forces in the composite layers. FSDT is chosen for its ability to accurately account for transverse shear deformation effects, significant in thick composite laminates [24]. The TDOF approach, coupled with a nonlinear Hertz contact force model, offers a realistic representation of impact dynamics, including interactions between the impactor and the composite target [25]. Experimental validation is conducted using an INSTRON CEAST 9350 impact test system, with tests performed at different energy levels to simulate various impact scenarios.

The study evaluates the model's predictions against experimental results to determine its accuracy, reliability, and identifying limitations such as its inability to effectively simulate material damage. By validating this analytical model, the research seeks to establish a dependable tool for engineers and researchers to more precisely predict the impact behavior of composite materials [26]. The novelty of this study lies in in the multi-

level experimental validation, its computational efficiency and practical applicability. Unlike conventional numerical simulations, which are computationally intensive, this research develops and validates a simplified analytical model that accurately predicts the impact response of unidirectional (UD) CFRP composites. Besides that, it offers practical benefits by reducing the need for extensive experimental testing. This approach enables faster predictions and reducing the costs, making it a viable alternative for early-stage design assessments, particularly in aerospace, automotive, and defense applications. Furthermore, by systematically evaluating model performance across different energy levels, this study provides a deeper understanding of how well analytical approaches capture impact behavior, particularly in low-velocity impact scenarios.

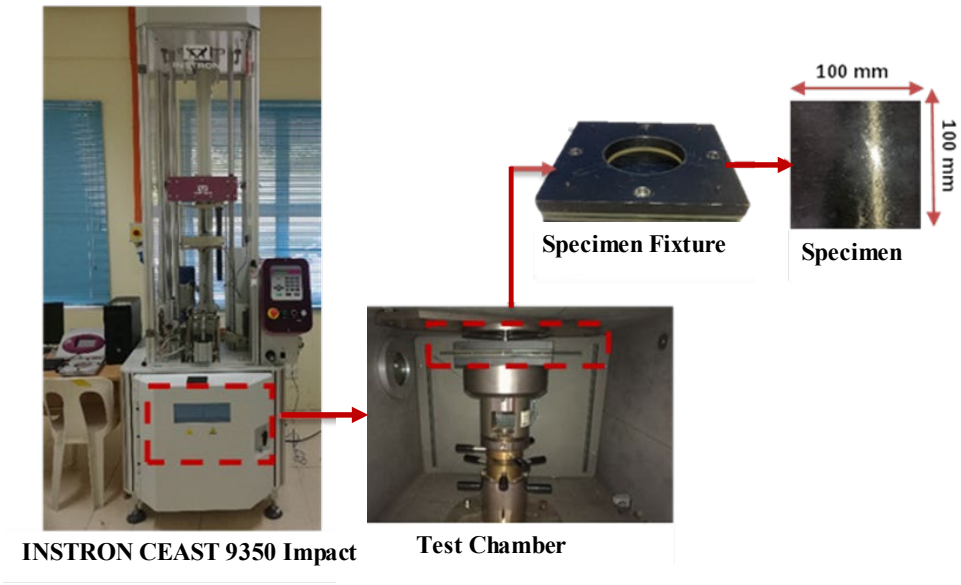

Figure 1: Impact damage test setup and UD CFRP specimen

2.0 EXPERIMENTAL PROCEDURE

To evaluate the accuracy of the analytical model, a series of experiments were conducted on UD CFRP composites subjected to low-velocity impacts. The specimens were fabricated using the vacuum infusion process which used vacuum pressure to drive the resin into a laminate [27].

Twelve specimens were prepared, each consisting of eight layers of laminated UD CFRP/Epoxy-1006 arranged in a $[0/90/0/90]_s$ stacking sequence. The panels measured 100 × 100 × 3 mm³, with each individual ply thickness of 0.375 mm. The impact tests were carried out using Instron CEAST 9350 impact test system, renowned for its precision in impact testing and ability to provide reliable data for validating analytical models [28].

The impact tests were employed using a hemispherical impactor tip with a diameter of 16 mm. A total impactor mass of 5.2 kg at velocities of 1.5 m/s, 2 m/s, and 2.5 m/s were employed in accordance with ASTM D7136 standards [29], which is corresponding to energy levels of 5.6 J, 10.3 J, and 16.14 J, respectively. Due to the non-standard sample size, a custom designed test rig was used to secure the specimens using circular clamps with rubber tips, as shown in Fig. 1.

Initial velocity was recorded using a grating velocimeter, while the impact force and displacement were measured via a load sensor integrated into the test setup. These experimental results will be used to compare with the analytical predictions for validation

purposes. The specimen configurations and material properties of the UD CFRP composites and the impactor properties are summarized in Table 1.

3.0 ANALYTICAL MODEL OF LOW VELOCITY IMPACT

In this study, an analytical undamaged model was developed to reliably predict impact force, displacement, and absorbed energy in UD CFRP composites under impact conditions. The methodology integrates advanced theoretical frameworks, numerical solution techniques, and experimental validation to ensure accurate predictions of these parameters. The model uses simple support boundary conditions and FSDT to accurately approximate the mechanical properties of the composites. FSDT provides a robust framework for modeling the shear deformation effects in thick composite laminates, improving the accuracy of impact predictions [30].

Hamilton's principle was applied to derive the governing equations of motion and the corresponding boundary conditions. To estimate impact parameters such as force, displacement, and absorbed energy, a modified spring-mass system with TDOF and a nonlinear Hertz contact force model was implemented. This approach improves the realism of the impact dynamics simulation by accurately capturing the interaction forces and system response [31]. The impact forces were modeled as being concentrated on a specific patch area. Analyses were conducted at different energy levels, and the results were compared with experimental data from the literature, showing acceptable agreement. Further validation was achieved by comparing the analytical results with experimental tests performed on UD CFRP composites, confirming the model's reliability in predicting the dynamic behavior of composite materials under impact conditions.

Table 1: The geometrical and mechanical properties of UD CFRP composites [32]

Specimen Properties	**Value**
Size	100 × 100 × 3 mm^3
Stacking sequence	[0/90/0/90]s
Ply thickness	0.375 mm
Boundary Condition	Simply supported
Mechanical Properties of UD CFRP Composites	
E_1	130 GPa
E_2, E_3	7.6 GPa
G_{23}	3.2 Gpa
G_{12}, G_{13}	3.8 Gpa
v_{12}, v_{13}	0.33
v_{23}	0.35
Density	1600 kg/m^3
Mechanical Properties of Impactor (Steel)	
E_1	200 GPa
Poisson's ratio	0.3
Density	7971 kg/m^3
Diameter	16 mm
Mass	5.2 kg

3.1 Formulation of Governing Equations

The low-velocity impact (LVI) on UD CFRP composites is illustrated in Figure 2. The impactor is rigid and spherical, while the plate is a simply supported rectangular one with dimensions of a × b × h. Whitney and Pagano developed the governing equations for composite laminate flat plates, as shown in Equation 1 [33]:

$$u = u^0(x,y,t) + z\Psi_x(x,y,t);\quad v = v^0(x,y,t) + z\Psi_y(x,y,t);\ \ w = w^0(x,y,t) \qquad (1)$$

In this context, u^0, v^0 and w^0 represent the plate displacements along x, y and z directions at the mid-plane, while $\Psi_x$and Ψ_y denote the shear rotations in the x and y directions.

For the especially orthotropic form (B_{ij} =0, $A_{16} = A_{26} = D_{16} = D_{26} = 0$), the governing equations are:

$$D_{11}\Psi_{x,xx} + D_{66}\Psi_{x,yy} + (D_{12} + D_{66})\Psi_{y,xy} - K_{sh}A_{55}\,\Psi_x - K_{sh}A_{55}\,\Psi_{,x} = I\Psi_x \qquad (2)$$

$$(D_{12} + D_{66})\Psi_{x,xy} + D_{66}\Psi_{y,xx} + D_{22}\Psi_{y,yy} - K_{sh}A_{44}\,\Psi_y - K_{sh}A_{44}\,\Psi_{,y} = I\Psi_y \qquad (3)$$

$$K_{sh}A_{55}\Psi_{x,x} + K_{sh}A_{55}W_{,xx} + K_{sh}A_{44}\,\Psi_{y,y} + K_{sh}A_{44}\,\Psi_{,yy} + q = \rho W \qquad (4)$$

In this case, K_{sh} represent the shear correction factor, typically equals to $\pi^2/12$, while q denotes the dynamic normal load acting on the plate. Additionally:

$$(A_{ij}, B_{ij}, D_{ij}) = \int_{-\frac{h}{2}}^{\frac{h}{2}} Q_{ij}^k + (I, Z, Z^2)d_Z;\ (\rho, I) = \int_{-\frac{h}{2}}^{\frac{h}{2}} \rho_0\,(I, Z^2)d_Z \qquad (5)$$

Here, ρ_0 denotes the density of each layer, while ρ represents the total density of the plate. I is the moment of inertia, and h is the plate thickness. The terms (Q_{ij}^k) $(for\ i,j = 1,2,6)$ correspond to the reduced in-plane stiffness components, whereas (Q_{ij}^k) $(for\ i,j = 4,5)$ represent the reduced transverse shear stiffness components, as described by Whiteny and Pagano [33]. A simply supported square plate with dimensions ***a*** and ***b,*** is selected for analysis, subject to the following boundary conditions:

$$w = \Psi_{x,x} = \Psi_y = 0\ ;\ at\ \ x = 0\ , a \qquad (6)$$

$$w = \Psi_{y,y} = \Psi_x = 0\ ;\ at\ \ y = 0\ , b \qquad (7)$$

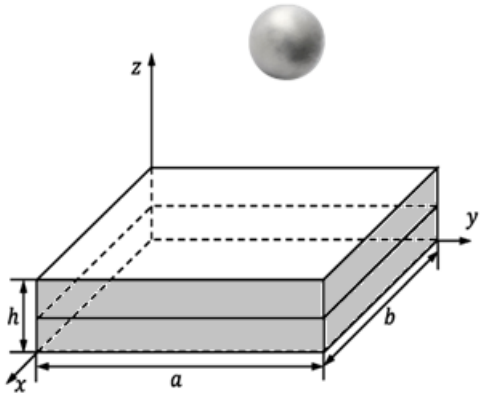

Figure 2: Illustration of UD CFRP composite impacted by a spherical mass.

3.2 Constitutive Equations

The constitutive equations for the on-axis stress-strain relationship for an orthotropic material of a flat plate composite as described in [30] are as follows:

$$\begin{bmatrix}\sigma_1\\ \sigma_2\\ \tau_{12}\end{bmatrix}=\begin{bmatrix}K_{11} & K_{12} & 0\\ K_{12} & K_{22} & 0\\ 0 & 0 & K_{66}\end{bmatrix}\begin{bmatrix}\varepsilon_1\\ \varepsilon_2\\ \gamma_{12}\end{bmatrix} \tag{8}$$

$$\begin{bmatrix}\tau_{13}\\ \tau_{23}\end{bmatrix}=\begin{bmatrix}K_{44} & 0\\ 0 & K_{55}\end{bmatrix}\begin{bmatrix}\gamma_{23}\\ \gamma_{13}\end{bmatrix} \tag{9}$$

In these equations, σ represents the stresses in the principal directions, while ε denotes the corresponding strains, The matrices K_{ij} signify the reduced stiffness matrices of the composite plate structure. The constitutive equation can be derived by expressing the force-couple resultants in terms of stresses and integrating through the plate thickness, leading to:

$$\begin{bmatrix}N\\ M\end{bmatrix}=\begin{bmatrix}A_{ij} & B_{ij}\\ B_{ij} & D_{ij}\end{bmatrix}\begin{bmatrix}\varepsilon^0\\ k\end{bmatrix};\ \ i,j=1,2,6 \tag{10}$$

$$[S]=\left[K_{sh}A_{ij}\right][\gamma];\ \ i.j=4,5 \tag{11}$$

Here, N and S represent the force vectors, while M denotes for the moment vectors. The terms A_{ij} ,B_{ij} and D_{ij} correspond to the components of the extensional, coupling, and bending stiffness matrices, respectively. Additionally, ε^0 and k represent the laminate middle plane strain vector and laminate middle plane curvature vector, respectively, while K_{sh} is the shear correction factor.

3.3 Contact Force Analysis

A two-degrees of freedom springs-mass model was utilized by [31] to calculate the impact force, as illustrated in Figure 3. The corresponding equation of motion are:

$$m_i\ddot{z}_i+F=0\ ;\ \ m_p\ddot{z}_p+K_{bs}z_i+K_lz_i^3-F=0 \tag{12}$$

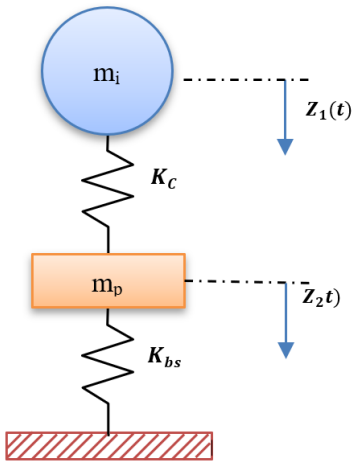

Figure 3: Illustration of two-degrees of freedom springs-masses model

Applying Hertz's contact law, the impact force is expressed as:

$$F(t)=K_c\delta^n \tag{13}$$

In the modified Hertz's contact law, the impact force between the metallic impactor and the impacted surface of the targeted area of the composite plate structure during the impact

can be governed by the non-linear power-law of Eq (13). δ is the relative indentation between the impactor and the impacted surface of the target structure, K_C is Hertz's contact stiffness, and the indentation is defined by:

$$\delta(t) = Z_1(t) - Z_2(t) \tag{14}$$

Here, $Z_1(t)$ represents the displacement of the impactor, while $Z_2(t)$ denotes the transverse displacement of the impacted surface at the impact location (x_1, x_2). In this analysis, the indentation of the impacted surface is assumed to follow the Hertzian contact law for a half-space. The equation of motion for the impactor is given in Eq (12), where Mi is the mass of the impactor, and F represent the contact forces between the impactor and the target structure (middle of the plate).

3.4 Deflection and Stress-Strain Analysis

By transforming the system of ordinary differential equations into a second-order form in time for the Fourier coefficients of the transverse deflection, the equation of motion for the composite plate under a point load *q(x, y, t)* can be expressed as [34]:

$$\begin{bmatrix} L_{11} & L_{12} & L_{13} \\ L_{12} & L_{22} & L_{23} \\ L_{13} & L_{23} & L_{33} \end{bmatrix} \begin{bmatrix} A_{mn}(t) \\ B_{mn}(t) \\ W_{mn}(t) \end{bmatrix} = \begin{bmatrix} 0 \\ 0 \\ P_{mn}(t) - \rho h \overline{W}_{mn}(t) \end{bmatrix} \tag{15}$$

Where the L_{ij} coefficients are defined by:

$$q(x, y.t) = \sum_m \sum_n P_{mn}(t) \sin\left(\frac{m\pi}{a}x\right) \sin(\frac{n\pi}{b}y) \tag{16}$$

For a concentrated load applied at the point (x_c, y_c), $P_{mn}(t)$ represents the terms of the Fourier series.

$$P_{mn}(t) = \frac{4F(t)}{ab} \sin\left(\frac{m\pi}{a}x_c\right) \sin(\frac{n\pi}{b}y_c) \tag{17}$$

The impact response of a rectangular plate with simply supported boundary conditions is assumed to take the following form [34]:

$$\psi_x(x, y, t) = \sum_{mn=1}^{\infty} A_{mn}(t) cos\left(\frac{m\pi}{a}x\right) \sin\left(\frac{n\pi}{b}y\right) \tag{18}$$

$$\psi_y(x, y, t) = \sum_{mn=1}^{\infty} B_{mn}(t) sin\left(\frac{m\pi}{a}x\right) cos\left(\frac{n\pi}{b}y\right) \tag{19}$$

$$W(x, y, t) = \sum_{mn=1}^{\infty} W_{mn}(t) sin\left(\frac{m\pi}{a}x\right) \sin\left(\frac{n\pi}{b}y\right) \tag{20}$$

The equations $W_{mn}(t) + \omega_{mn}^2 W_{mn}(t) = \frac{P_{mn}(t)}{\rho h}$ are solved Using the MATLAB software and based on the Runge-Kutta method to calculate the values of $W_{mn}(t), \Psi_x$ and Ψ_y. A numerical method based on FSDT is utilized to evaluate the contact force between the impactor and the composite laminate.

4.0 RESULTS AND DISCUSSION

This study evaluates the impact behavior of UD CFRP composites by comparing predictions from analytical model with experimental data across three energy levels which are 5.6 J (C1), 10.3 J (C2) and 16.14 J (C3). Unlike many existing analytical models, which remain unverified or rely solely on numerical approximations, this study provides a direct experimental validation, strengthening its credibility and practical applicability. The analytical model's predictions were compared with experimental data to assess its accuracy and identify areas for improvement.

4.1 Impact Force-Time Analysis

For the force-time curves presented in Figure 4, the model demonstrated strong agreement at lower energy levels. At C1 (5.6 J), the experimental results showed a rapid increase to a peak force of 2,763 N, followed by a gradual decline as energy was absorbed. The model predicted a similar trend, with a peak force of 2,851 N and an error of only 3%. However, the model underestimated the force deterioration, suggesting the need to improve its ability to simulate energy dissipation mechanisms such as damping. At C2 (10.3 J), the experimental peak force increased to 3,949 N, with a plateau phase indicating material deformation. While the model accurately predicted the peak force at 3,891 N, with a negligible error of only 1%, it failed to capture the plateau behavior, highlighting challenges in modelling complex material responses at moderate energy level. At the highest energy level, C3 (16.14 J), the experimental peak force was 3,364 N, with sustained force duration indicating significant energy absorption. The model overestimated this peak force by 45% at 4,888 N, which underscores its limitations in simulating high-energy impact dynamics and more complex damage mechanisms such as fibers rupture, matrix cracking, delamination, and debris accumulations [11, 35].

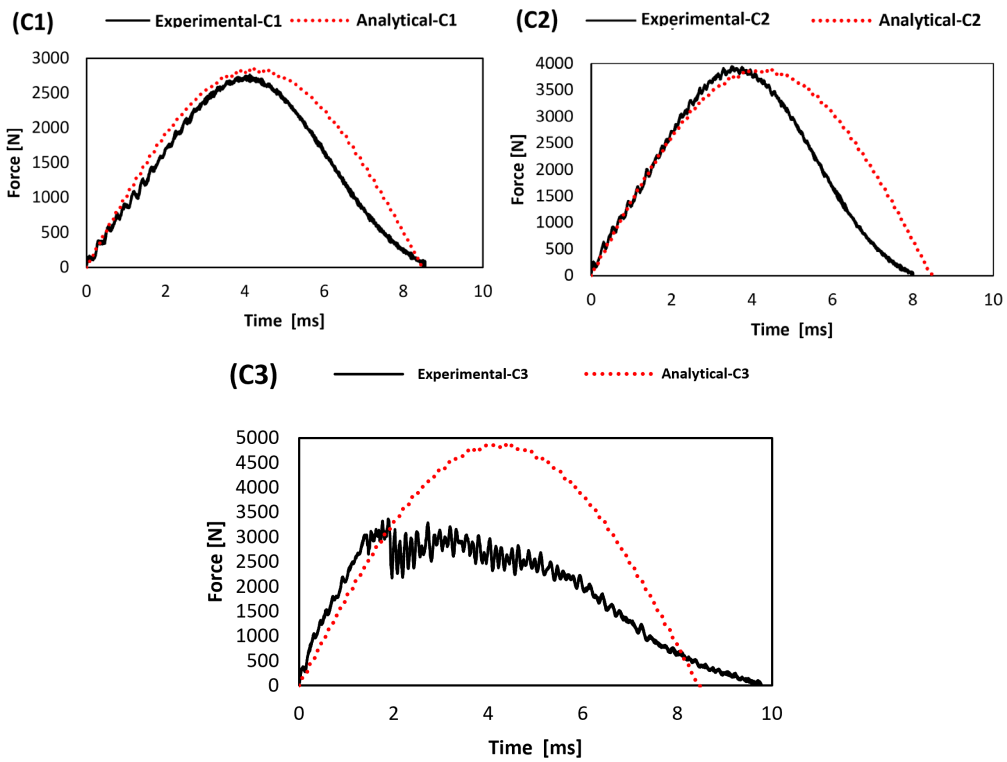

Figure 4: Time-history curves showing the variation of impact force at each energy level

4.2 Displacement-Time Analysis

The displacement-time analysis revealed similar trends as presented in Figure 5. At C1 (5.6 J), the experimental maximum displacement was 4.2 mm, while the model underestimated this value at 3.75 mm, resulting in an error of 11%, which was likely due to simplifications in material stiffness and boundary condition assumptions. At C2 (10.3 J), the experimental peak displacement increased to 5.24 mm, with the model closely predicting 5.12 mm, underestimating about 2%, indicating a need to adjust for material nonlinearities and rate-dependent effects. At C3 (16.14 J), the experimental peak displacement reached 7.13 mm, while the model underpredicted this value at 6.43 mm, reflecting a 10% error, reflecting limitations in simulating complex behaviors like damage initiation and progression [36-37].

4.3 Energy-Time Analysis

Figure 6 shows the energy-history analysis of all three impact energies. It shows that the model performed well in predicting absorbed energy at all energy levels, albeit with slight underestimations at higher energies. At C1, the experimental absorbed energy reached maximum at 5.6 J, with the model predicting 5.35 J and a 4% error. At C2 and C3, the model underpredicted absorbed energy with values of 9.96 J and 15.72 J, respectively, both within a 3% error margin, suggesting enhancements are needed to simulate dynamic interactions and nonlinear. While the results demonstrate the model's ability to capture overall energy absorption trends, its accuracy decreases as damage mechanisms like matrix cracking, fiber ruptures, and delamination become more significant at higher energy.

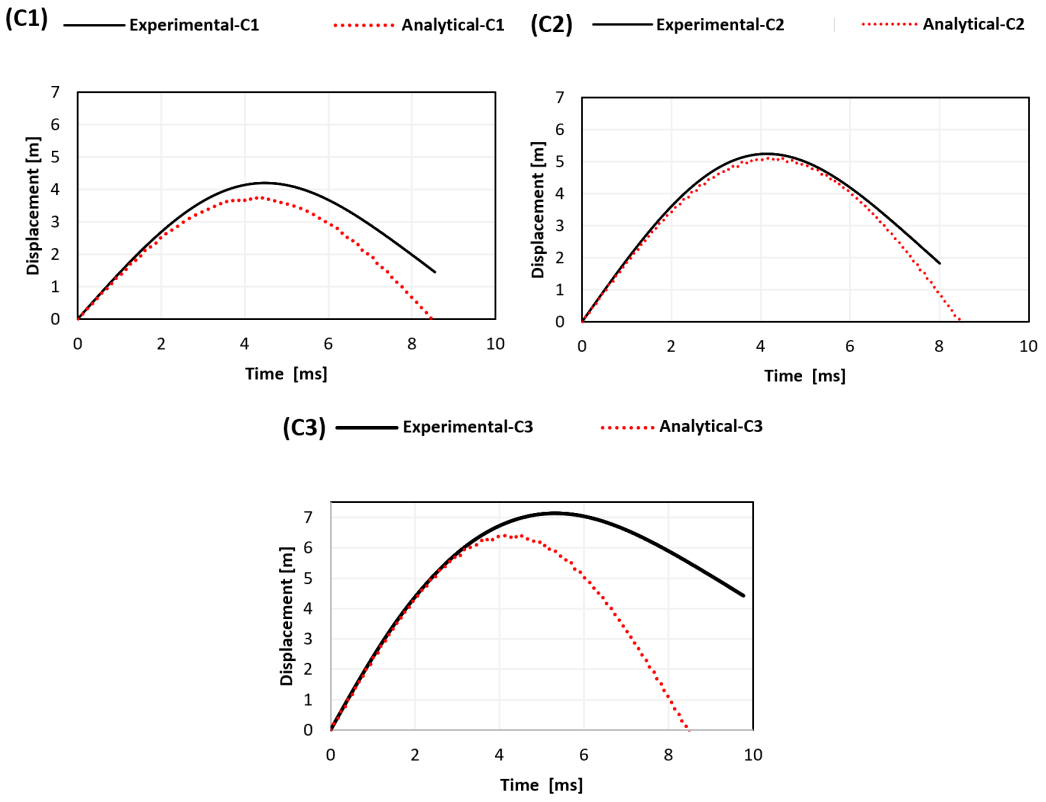

Figure 5: Time-history curves showing the variation of displacement throughout the impact event at each energy level

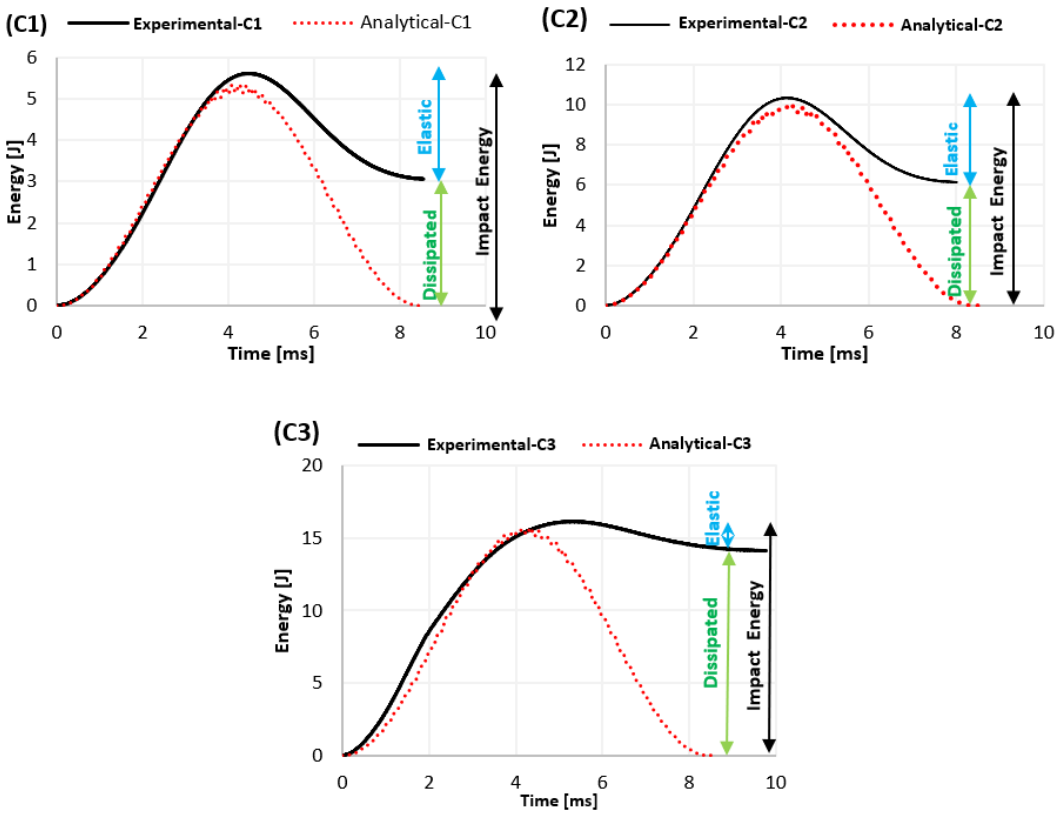

Figure 6: Time-history curves illustrating the absorption and variation of energy during impact at each energy level

4.4 Impact Force-Displacement Analysis

The force-displacement analysis as shown in Figure 7 emphasized further the model's strengths and weaknesses. At C1, the force-displacement relationship was relatively linear, indicating elastic behavior with a maximum force of 2,763 N and displacement of 4.2 mm. In this case, the model accurately predicts this linear relationship, aligning well with experimental observations. At C2 and C3, experimental data revealed nonlinear behavior due to damage mechanisms. The model captured the initial elastic trend but underestimated peak displacement and failed to replicate nonlinear deformation, underscoring the need for advanced material modeling to account for plasticity and damage progression.

Table 2 presents a summary of the overall results derived from Figure 4 through Figure 7, along with the error analysis comparing the analytical model to experimental data. It clearly shows that larger errors are observed for C3 specimens that are being impacted with higher levels of energy. From the literature perspective, CFRP plates that subjected to low velocity impacts of more than 15J and above typically experience multiple damage mechanisms in the impacted region like matrix cracking, delamination, fiber fracture, etc. Figure 8 illustrates an example of these damage mechanisms in the impacted area, based on an investigation by Israr et al [35]. Their study revealed that, in addition to several damage mechanisms, there is also plenty of debris present in the delaminated areas resulting from the ruptures of the fibres. This debris blocks the fibres and matrices of the impacted specimen, preventing them from returning to their original positions. Consequently, this condition affects the relaxation of indentation and the absorbed energy [35]. These effects have not yet considered in the developed analytical model, which explains the discrepancies, particularly at higher impact energies.

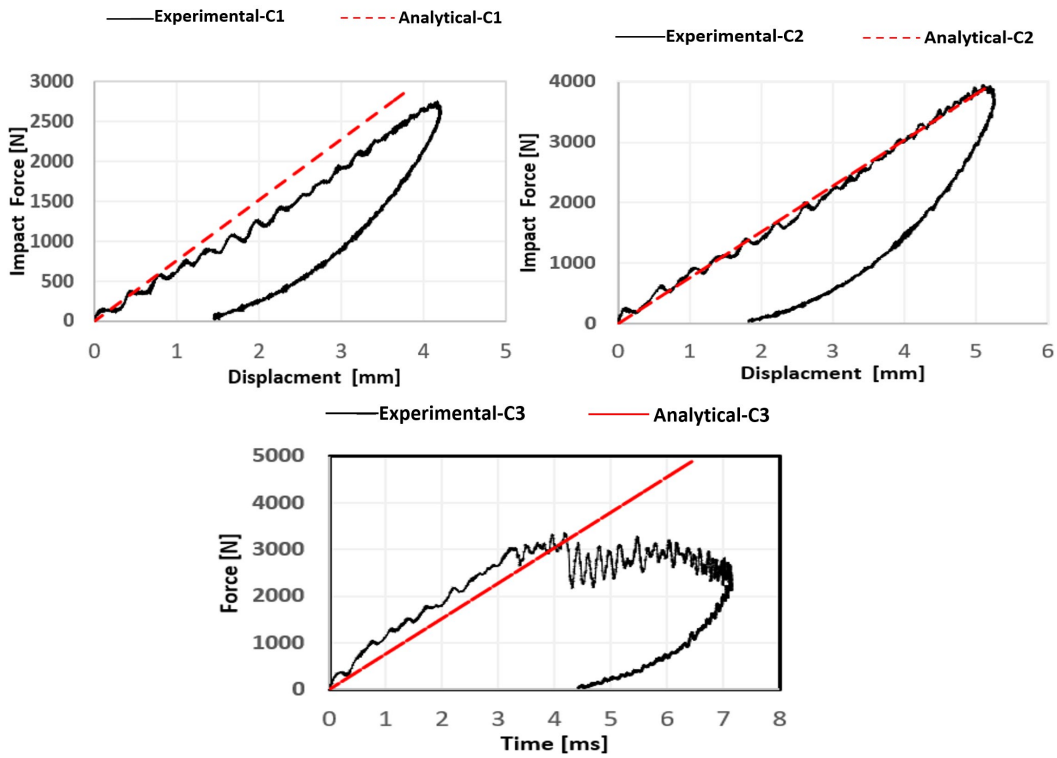

Figure 7: Force-displacement curves showing the mechanical response at each energy level

Table 2 Summary of analytical model predictions and experimental test results of UD CFRP composite under low-velocity impact at varying impact energies

Parameter	C1	C2	C3
Max Impact Force [N]			
Experimental	2,763	3,949	3,364
Analytical	2,851	3,891	4,888
Error	3%	-1%	45%
Max Displacement [mm]			
Experimental	4.2	5.24	7.13
Analytical	3.75	5.12	6.43
Error	-11%	-2%	-10%
Indentation	1.5	1.9	4.4
Max Energy [J]			
Experimental	5.6	10.3	16.14
Analytical	5.35	9.96	15.72
Error	4%	3%	3%
Damage Energy	3.05	6.13	14.1
Absorbed Energy	2.55	4.17	2.04

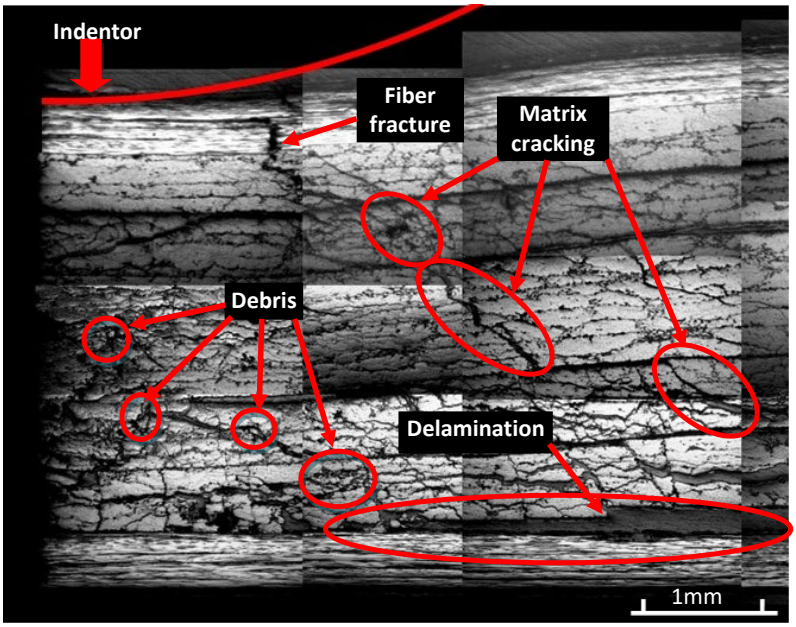

Figure 8: Example of the complex damage mechanisms near to the impacted area and the trap debris inside the delamination areas and matrices cracking [35]

5.0 CONCLUSION

The analytical model developed in this study serves as an effective tool for predicting the impact behaviour of UD CFRP composites, particularly under low-velocity impact conditions. It demonstrates good agreement with experimental results at lower energy levels, where the responses are mostly elastic. The model accurately predicts peak impact forces and energy absorption, particularly for the lowest energy level (C1), where discrepancies between the model and experimental results were minimal. This demonstrates the model's suitability for applications involving minimal deformation and limited damage.

One of the key contributions of this work is the multi-level experimental validation, which confirms the reliability of the model for simple impact scenarios. However, as impact energy increases, the model shows limitations. It struggles to simulate nonlinear responses and fails to fully capture complex damage mechanisms such as matrix cracking dan delamination. At higher energy levels (C2 and C3), the analytical model tends to overestimate peak forces and underestimate displacements.

These limitations highlight the need for more advanced material modelling. Incorporating damage progression and strain-rate effects would improve prediction accuracy and make the model more robust for a wider range of conditions. This would also enhance its usefulness in designing composite structures for safety-critical industries like aerospace and automotive.

While the model cannot fully replace experimental testing, it serves as a valuable complement. It enables rapid assessments and helps identify trends in energy absorption, displacement, and impact forces. By reducing the need for extensive testing, the model supports more efficient design processes and cost savings.

In conclusion, this study contributes to the field of composite impact modelling by providing a reliable, computationally efficient tool. Future improvements should focus on integrating damage mechanics and nonlinear behaviour to bridge the gap between analytical predictions and real-world performance. These advancements will support the

development of innovative composite solutions, optimizing performance and safety across various engineering applications.

ACKNOWLEDGEMENT

The authors sincerely appreciate the financial support provided by the Ministry of Higher Education through the Fundamental Research Grant Scheme (FRGS), no. FRGS/1/2022/TK10/UTM/02/27 (R.J130000.7851.5F517) as well as Universiti Teknologi Malaysia under UTMFR grant, Q.J130000.3851.21H92.

REFERENCES

1. Alshammari B. A., Alsuhybani M. S., Almushaikeh A. M., Alotaibi B. M., Alenad A. M., Alqahtani N. B. and Alharbi A. G., 2021. Comprehensive Review of the Properties and Modifications of Carbon Fiber-Reinforced Thermoplastic Composites, *Polymers,* 13(15): 2474
2. Das M., Sahu S., and Parhi D.R., 2021. Composite Materials and Their Damage Detection using AI Techniques for Aerospace Application: A Brief Review, *Materials Today Proceedings*, 44(1): 955-960.
3. Jokinen J. and Kanerva M., 2019. Simulation of Delamination Growth at CFRP-Tungsten Aerospace Laminates Using VCCT and CZM Modelling Techniques, *Applied Composite Materials*, 26: 709–721.
4. Mohammadi R., Najafabadi M.A., Saghafi H., Saeedifar M., and Zarouchas D., 2021. The Effect of Mode II Fatigue Crack Growth Rate on the Fractographic Features of CFRP Composite Laminates: An Acoustic Emission and Scanning Electron Microscopy Analysis, *Engineering Fracture Mechanics*, 241: 107408.
5. Gibson R. F. (2016). *Principles of Composite Material Mechanics*, CRC Press, Boca Raton, United States.
6. Israr H. A., Chwen T. S., Latif A. A., Wong K. J., Koloor, S. S. R., Yidris N., and Yahya M. Y., 2022. Preliminary Structural Design of Coreless Spoiler by Topological Optimization, *Processes*,10: 2076.
7. Kim J. H., Kim S. K. and Kim H. S., 2015. Enhanced Fuel Efficiency and Reduced Emissions of Aircraft Through the Use of CFRP Materials, *Aerospace Science and Technology*, 46: 525-531.
8. Johnston J. P., Koo B., Subramanian N. and Chattopadhyay A., 2017. Modeling the Molecular Structure of the Carbon Fiber/Polymer Interphase for Multiscale Analysis of Composites. *Composites Part B: Engineering*, 111: 27–36.
9. Garoz Gómez D., Pascual-González C., García-Moreno C. J. and Fernández-Blázquez J. P., 2023. Methodology to Design and Optimise Dispersed Continuous Carbon Fibre Composites Parts by Fused Filament Fabrication, *Composites Part A: Applied Science and Manufacturing*, 165: 107315
10. Li M., Zhang H., Li S., Zhu W. and Ke Y., 2022. Machine Learning and Materials Informatics Approaches for Predicting Transverse Mechanical Properties of Unidirectional CFRP Composites with Microvoids, *Materials & Design*, 224: 111340.
11. Hongkarnjanakul N., Bouvet C., and Rivallant S., 2013. Validation of low velocity impact modelling on different stacking sequences of CFRP laminates and influence of fibre failure. *Composite Structures,* 106: 549–559.
12. Bieniaś J., Jakubczak P., Surowska B. and Dragan K., 2015. Low-energy Impact Behaviour and Damage Characterization of Carbon Fibre Reinforced Polymer and Aluminium Hybrid Laminates, *Archives of Civil and Mechanical Engineering*, 15(4): 925–932.
13. Luo Z., Wang H., Ng C.T., Fu J., Zhang Z. and Wang C., 2024. On The Low-velocity Impact Properties of CFRP/HAFRP Interlayer Hybrid Fibre Composite Laminates, *Engineering Structures,* 315: 118387
14. Bianco G. D., Giammaria V., Capretti M., Boria S., Lenci S., Ciardiello R. and Castorani V., 2024. Low-Velocity Impact of Carbon, Flax, and Hybrid Composites: Performance Comparison and Numerical Modeling, *Composite Structures*, 344: 118318
15. Cengiz A., Yildirim I. M. and Avcu E., 2024. Flexural and Low Velocity Impact Behaviour of Hybrid Metal Wire Mesh/Carbon-Fibre Reinforced Epoxy Laminates, *Composites Communications*, 46: 101844
16. Hakim M. L., Nafianto R., Nugraha A. D., Wiranata A., Supriyanto E., Nugroho G. and Muflikhun M. A., 2024. Advanced FEA Simulation of GFRP and CFRP Responses to Low Velocity Impact: Exploring Impactor Diameter Variations and Damage Mechanisms, *Composite Part C: Open Access*, 15: 100541
17. Strugala G., Klugmann M., Landowski M., Szkodo M. and Mikielewicz D., 2018. A Universal NDT Method for Examination of Low Energy Impact Damage in CFRP with the Use of TLC Film, *Nondestructive Testing and Evaluation*. 33(3): 315–328.
18. Vescovini A., Li C. X., Malverti C., Jin B. C. and Manes A., 2025. Low-velocity Impact Behavior of Flat and Tapered Single–Double Composites Specimens, *Composite Structures*, 335: 118823
19. Li F., Jin S., Li W. and Luo Z., 2024. Assessment of Damage Prediction Models for Composite Laminates under Single and Repeated Low-Velocity Impacts, *Aerospace Science and Technology*, 155: 109633

20. Zhang Z., Zhang K., Zhang G. and Zheng B., 2024. Low-velocity Impact Simulation of Carbon Fiber Reinforced Composite Laminate using IFF-Criterion Based on BP-ANN, *Aerospace Science and Technology*, 148: 109095
21. Liu J., Li Y., Huang M., Zhang Y., Lu Y. and Dong L., 2024. Prediction of Low-Velocity Impact Mechanical Response and Damage in Thermoplastic Composites Considering Elastoplastic Behavior, *International Journal of Impact Engineering*, 194: 105099.
22. Li H., Li P., Li Z., Xiong J., Zhou B., Zhang H., Bai H., Wang S., Wang X., Cao H., Sun W., Han Q., Zhou J. and Guan Z., 2024. Analytical Modeling and Analysis of The Low-Velocity Penetration and Non-Penetration Behaviors of Fiber-Reinforced Composite Cylindrical Shells Based on Critical Impact Velocity Criterion, *International Journal of Impact Engineering*, 186: 104858.
23. Singh A. K., Davidson B. D., Zehnder A. T., and Hasseldine B. P. J., 2017. An Analytical Model for The Response of Carbon/epoxy-Aluminum Honeycomb Core Sandwich Structures under Quasi-Static Indentation Loading, *Journal of Sandwich Structures & Materials*, 21(6): 1930–1952.
24. Arachchige B., Ghasemnejad H. and Augousti A. T., 2016. Theoretical Approach to Predict Transverse Impact Response of Variable-Stiffness Curved Composite Plates, *Composites Part B: Engineering*, 89: 34–43
25. Salami S. J., and Dariushi S., 2018. Geometrically Nonlinear Analysis of Sandwich Beams under Low Velocity Impact: Analytical and Experimental Investigation, *Steel and Composite Structures*, 27(3): 273–283.
26. Wolniak M., Hofmeister B., Jonscher C., Fankhänel M., Loose A., Hübler C. and Rolfes R., 2023. Validation of An FE Model Updating Procedure for Damage Assessment using a Modular Laboratory Experiment with a Reversible Damage Mechanism, *Journal of Civil Structural Health Monitoring*, 13(6–7): 1185–1206
27. Ouezgan A., Mallil E. H. and Echaabi J., 2022. Manufacturing Routes of Vacuum Assisted Resin Infusion: Numerical investigation, *Journal of Composite Materials*, 56(21): 3221–3236.
28. Ameerul M., Mohsin A., Iannucci L., Greenhalgh E. S., Chirdon W., and Khattab A., 2021. Experimental and Numerical Analysis of Low-Velocity Impact of Carbon Fibre-Based Non-Crimp Fabric Reinforced Thermoplastic Composites, *Polymers,* 13(21): 3642
29. ASTM D7136/D7136M. 2007. Standard Test Method for Measuring the Damage Resistance of a Fiber-Reinforced Polymer Matrix Composite to a Drop-Weight Impact Event.
30. Reddy J. N., 2003. Mechanics of Laminated Composite Plates and Shells: Theory and Analysis, Second Edition, CRC Press, Boca Raton, Florida, United States
31. Payeganeh G. H., Ashenai Ghasemi F. and Malekzadeh K., 2010. Dynamic Response of Fiber–Metal Laminates (FMLs) Subjected to Low-Velocity Impact, *Thin-Walled Structures*, 48(1): 62–70.
32. Zhou J., Liu B., and Wang S., 2022. Finite Element Analysis on Impact Response and Damage Mechanism of Composite Laminates under Single and Repeated Low-Velocity Impact, *Aerospace Science and Technology*, 129: 107810
33. Whitney J. M., and Pagano N. J., 1970. Shear Deformation in Heterogeneous Anisotropic Plates, *Journal of Applied Mechanics*, 37(4): 1031–1036.
34. Abrate S., 2011. Impact Engineering of Composite Structures, CISM Courses and Lectures, vol. 526, Springer Wein New York, United States.
35. Israr H. A., Hongkarnjanakul N., Rivallant S. and Bouvet C., 2014. Post-Impact Investigation of CFRP Laminated Plate, *Jurnal Teknologi*, 71(2): 71-78
36. Bouvet C., Rivallant S. and Barrau J. J., 2012. Low Velocity Impact Modeling in Composite Laminates Capturing Permanent Indentation, *Composite Science Technology,* 72(16): 1977–88
37. He W., Guan Z. and Li X., 2013. Prediction of Permanent Indentation due to Impact on Laminated Composites Based on An Elasto-Plastic Model Incorporating Fiber Failure, *Composite Structures,* 96: 232–242.